Journal of Applied Electrochemistry **32**: 157–164, 2002.

Tarnishing and corrosion of silver-based casting alloys in synthetic salivas of different compositions

M. FERNÁNDEZ LORENZO de MELE[1]* and G. DUFFÓ[2]
[1]*INIFTA, Facultad de Ciencias Exactas, Universidad Nacional de La Plata, C.C. 16, Suc. 4, 1900 La Plata, Argentina*
[2]*Departamento de Materiales, Comisión Nacional de Energía Atómica, Av. Del Libertador 8250 (1429), Buenos Aires, Argentina*
*(*author for correspondence, e-mail: mmele@inifta.unlp.edu.ar)*

Received 5 September 2001; accepted in revised form 18 October 2001

Key words: corrosion, palladium, silver, synthetic saliva, tarnishing

Abstract

The aim of this work is to study the electrochemical response of Ag and Ag-based alloys in synthetic salivas of different compositions. The effect of several anions present in saliva on the dissolution of Ag and some of the alloy components, such as Pd and Cu, was evaluated. Potentiostatic and potentiodynamic techniques were used and were complemented with atomic adsorption and XPS analysis. Chloride, fluoride and thiocyanate were particularly analysed because of their aggressiveness. Corrosion, pigmentation and/or tarnishing processes were enhanced when they were present in the synthetic saliva. A dependence of the selectivity of Pd dissolution from Ag–15Pd binary alloy with the potential was noticed. Ag microsegregations and precipitates formed on casting alloys showed higher activity than the matrix and rendered the alloy more susceptibility to deterioration. The need to use a normalised saliva to make comparisons of electrochemical results is highlighted.

1. Introduction

The characterisation of the *in vitro* corrosion and tarnishing behaviour of Ag-based casting alloys is both of fundamental and applied interest because corrosion not only affects the functionality and resistance of the biomaterials [1] but also may cause pathological phenomena. The corrosive dissolution of metal components from the dental materials within the body fluids may provide an excessive supply of trace elements to the patient's body [2–4]. Massive enrichment of insoluble toxic Ag corrosion products have been observed in the proximity of the metallic biomaterial, probably yielding to tissue irritation and localised bond damage [5, 6].

For *in vitro* corrosion tests, potentiodynamic polarisation analysis is frequently used as a screening method to elucidate the electrochemical behaviour of dental alloys on exposure to synthetic solutions [1, 2]. Cyclic polarisation has the additional advantage of providing information about the reduction of corrosion product layers. This technique is also useful to study the influence of microstructure on the corrosion resistance of the metal. In the case of Ag–Pd alloys the interpretation of polarisation curves made by different authors is not coincident and deserves further research [7, 8].

Synthetic solutions are usually employed when polarisation curves are performed because body fluids are unstable and often difficult to obtain in sufficient amounts. Table 1 summarised the concentrations of the main components of 16 salivas reported in other works [9–25]. The concentration of some of the aggressive anions such as Cl^- and SCN^- varies within a wide concentration range. Electrochemical characterisation of Ag-based casting alloys in synthetic salivas, Ringer's and NaCl solutions has revealed active–passive behaviour of this alloy, which depends on the electrolyte composition [1, 2, 6]. However, it is difficult to compare results obtained by different authors using different synthetic media.

The aim of this work is: (a) to study the electrochemical response of Ag and Ag-based casting alloys using potentiostatic and potentiodynamic techniques in synthetic saliva of different compositions; (b) to analyse the effect of several anions (chloride, thiocyanate, fluoride, phosphate) present in saliva on the metal corrosion of this alloys.

2. Experimental details

A conventional double-wall Pyrex glass electrolysis cell with three electrode compartments was used. The working electrodes consisted of a high purity Ag (99.99%) and Pd cylinders (0.25 cm diameter, 0.049 cm^2 exposed area, and 0.7 cm diameter, 0.38 cm^2, respectively); a type III Ag-based casting alloy (CAIII)

Table 1. Concentration (g l^{-1}) of the main components of several synthetic salivas

Component	Saliva[a]															
	E	J	FI	FII	FIII	B	To	Cm	O	TZI	TZII	D	C	Er	A	N
NaCl	0.7	0.85	0.4	0.4	0.4	6	0.67	0.7	0.85			1.5	0.86	0.58	0.7	
KCl	1.2	1.2	0.4	0.4	0.4	0.3	0.96	1.2	1.2	1.5	1.47					1.5
$NaHCO_3$	1.5							1.5		1.5	1.25	0.6		1.5	1.5	1.5
$CaCl_2 \cdot 2H_2O$		0.05	0.8	0.8	0.8	0.2	0.12	–	0.2				0.91	0.166		
NaH_2PO_4			0.69	0.78	0.69					0.5	0.19	0.56				0.5
KH_2PO_4	0.26						0.09							0.34	0.26	
K_2HPO_4		0.35						0.20	0.35							
Na_2HPO_4	0.26							0.26					1.0	0.34	0.19	
$MgCl_2$		0.05					0.04		0.05					0.014		
KSCN/NaSCN	0.33	0.1			0.3			0.33		0.5	0.52	0.2	0.07		0.33	0.5
NaF		0.01														
Na_2S			0.05	0.05						0.9		0.07				0.9
Lactic acid						3.1						0.8			0.13	
Urea	0.13		1	1	1			0.13								

[a] E (Ewers [10]), J (Jenkins [11]), FI (Fusayama [12]), FII (modified Fusayama II [13]), FIII (modified Fusayama III [14]), B (Barón [15]), To (Tomasi [16]), Cm (modified Carter [17]), O (Orthana [18]), TZI (modified Tani-Zuchi I [19]), TZII (modified Tani-Zuchi II [20]), D (Darwell [21]), C (Canivet [22]), Er (Ericsson [23]), A (Angelini [24]), N (Novak [25]).

(composition: Pd 1.88(±0.08)%, Cu 27(±1)%, Zn 8.5(±0.2)%, Sn 0.02–0.5%, Fe 0.005–0.02%, Ni 0.2–0.5% (0.5 cm diameter, 0.196 cm^2 exposed area)) axially embedded in an epoxy resin cylinder or a 0.08 cm diameter cylindrical wire of Ag–15Pd binary alloy (as-received). CAIII coupons were cast according to the manufacturer's recommendations. The working electrodes were firstly polished with emery paper of gradually decreasing grade (down to 600 grade), later with alumina paste (1 μm) and finally, successively rinsed with 96% ethanol and water. The counterelectrode was a large-area platinum sheet. A saturated calomel electrode (SCE) connected to the cell through a Lugging–Haber capillary tip was employed as reference electrode to which potentials are referred in the text. The electrolyte solutions consisted of (concentrations in grams per litre): synthetic saliva B [15] (NaCl: 6, KCl: 0.3, $CaCl_2$: 0.2, lactic acid: 3.1, (pH=6.5)); synthetic saliva Er [23] (NaCl: 0.58, Na_2HPO_4: 0.34, KH_2PO_4: 0.34, $KHCO_3$: 1.5, $MgCl_2$: 0.014, $CaCl_2$: 0.166, citric acid: 0.029); synthetic saliva E [10] (NaCl: 0.7, KCl: 1.2, KSCN: 0.33, Na_2HPO_4: 0.26, KH_2PO_4, $NaHCO_3$: 1.5, NH_2CONH_2: 0.13) and NaCl or KCl solutions of different concentrations between 0.016 and 1 M with and without the addition of NaF, $NaHCO_3$, KH_2PO_4 and KSCN. Solutions were deaerated with pure nitrogen.

Potentiodynamic cyclic runs were made at 20 mV s^{-1} in the $-1.0\ V < E < 0.8\ V$ potential range with different anodic and cathodic limits. Potentiostatic current transients at different pre-set potentials were also recorded. Electrochemical experiments were made at 37 °C. Occasionally potentiodynamic experiments at 0.5 mV s^{-1} and at room temperature were made.

Optical and scanning electron microscopic (SEM) observations of the electrodes before and after the electrochemical experiments were made.

The Pd profile in a Ag–15Pd alloy wire after polarisation in a chloride-containing solution was determined through XPS analysis. Prior to the analysis, the AgCl film anodically grown was dissolved in a concentrated NH_3 solution within an ultrasonic bath at room temperature during (at least) 10 min.

3. Results

The influence of the saliva composition on the electrochemical behaviour of Ag was studied in the −1.0–0.2 V potential range at 20 mV s^{-1} (Figure 1). Current levels close to zero can be observed up to 0.1 V, but, as the potential exceeds this value, the anodic current increases sharply. Anodic and cathodic processes are strongly

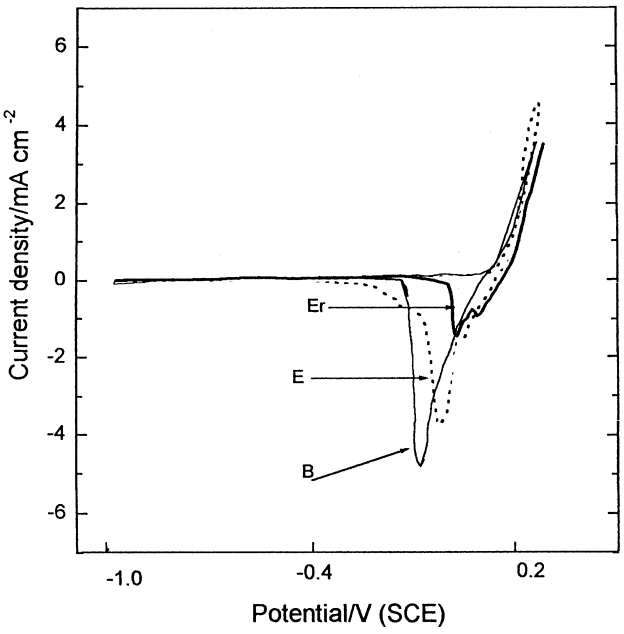

Fig. 1. Potentiodynamic cyclic polarisation curves at 20 mV s^{-1} with pure silver in salivas B, E and Er.

dependent on the saliva composition. The chloride level of the different solutions are the following – saliva B: 0.106 M, saliva Er: 0.016 M and saliva E: 0.028 M. The average chloride concentration in natural saliva [11] is close to that of saliva Er.

Three cathodic contributions can be detected in CAIII voltammogram in the case of saliva E (−0.25, −0.35, and −0.60 V, Figure 2) and two in the cases of salivas Er (a peak and a shoulder, Figure 3) and B. When

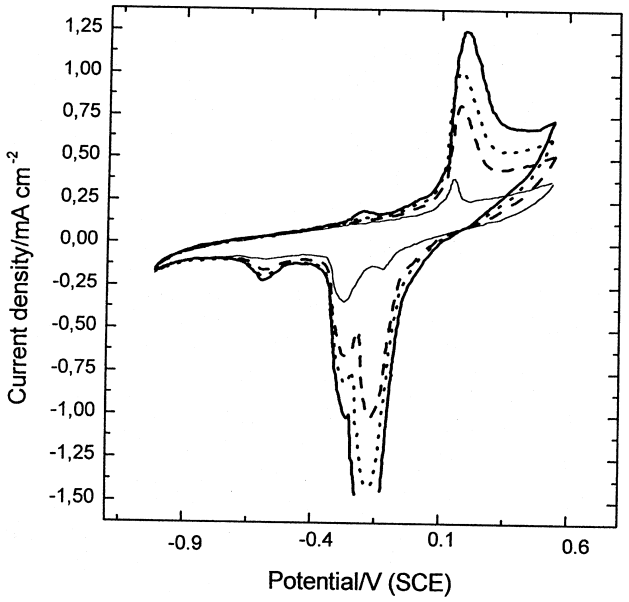

Fig. 2. Potentiodynamic cyclic polarisation curves at 20 mV s^{-1} with CAIII. Successive cycles were recorded in saliva E: (—) second cycle, (- - -) fifth cycle, (···) sixth cycle, (——) seventh cycle.

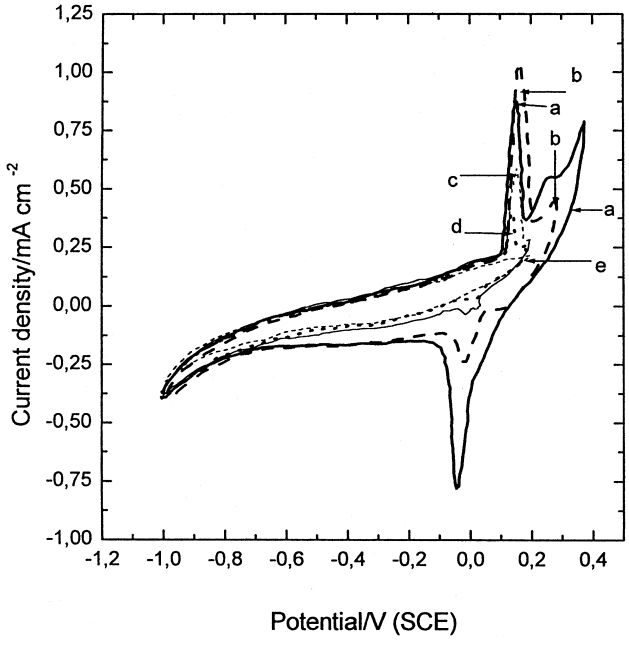

Fig. 3. Potentiodynamic cyclic polarisation curves at 20 mV s^{-1} with CAIII. Successive cycles were recorded in saliva E up to different anodic limits: 0.4 V (—); 0.3 V (- - -); first cycle up to 0.2 V (—); second cycle up to 0.2 V (···); 10th cycle up to 0.2 V (– – –).

successive potentiodynamic cycles are recorded in the −1.0–0.5 V potential range, several anodic contributions can be distinguished (Figures 2 and 3).

Current values increase markedly during successive cycles with CAIII in saliva E (Figure 2) but not with pure Ag. After several hours of cycling the anodic contributions overlap. The relationship between the height of the cathodic contributions also changes. After 5 h cycling period the shape of the curve resembles that of pure Ag with an additional contribution at −0.23 V. This potential is coincident with that corresponding to Cu_2O formation [26]. CAIII electrode looses its brightness during the experiment. Besides, according to the cathodic charge measurements, the real area of the electrode increases up to 2700 times the original one.

Interesting behaviour is observed when the anodic limit is decreased from 0.4 V (Figure 3, curve a) to 0.2 V (Figure 3, curves c–e). In the latter case the height of the peak at 0.15 V (peak I) decreases and then disappears after 10 successive runs between −1.0 and 0.2 V. The potential of peak I is similar to that corresponding to the Ag dissolution in pure Ag electrodes (Figure 1). Consequently, peak I is probably related to the dissolution of Ag deposited on the electrode during a previous cathodic scan. Thus, the following processes may occur on the electrode surface: at potentials higher than 0.3 V (Figure 3, curve a) Ag coming from the CAIII is dissolved and then reduced during the cathodic scan, forming a Ag layer on the electrode surface. This layer can be later oxidised at 0.15 V (peak I) during the following anodic scan. Obviously, during potential runs up to 0.2 V, the oxidation process at 0.3 V cannot occur and consequently the oxidation peak at 0.15 is inhibited (curves c–e).

3.1. *Influence of the anions on the electrochemical behaviour of Ag and Ag-based casting alloys*

3.1.1. *Effect of chloride*

Table 1 shows that the chloride concentration (the sum of chloride coming from KCl, NaCl, $MgCl_2$ and $CaCl_2$) of the synthetic salivas is very different. The height of the cathodic current peak increases from 5 mA cm^{-2} for a 0.028 M solution (like saliva E) to 30 mA cm^{-2} for a 0.16 M chloride solution (like that of Ringer's solution) (Figure 4a). The higher the chloride concentration the lower the potential at which the oxidation of Ag starts. It is interesting to note that current values are higher than those of synthetic salivas with the same chloride concentration (Figure 1, cathodic current peaks in salivas E and B: 3.8 and 5.7 mA cm^{-2} respectively). Thus, there is an inhibitory process associated to the other components of the salivas.

CAIII voltammograms (Figure 4b) are more complex than those of pure silver (Figure 4a). Several anodic and cathodic contributions, which increase when the concentration of chloride increases, can be detected when CAIII is used (Figure 4b). Particularly, when the chloride concentration is higher than 0.1 M, a current increase is

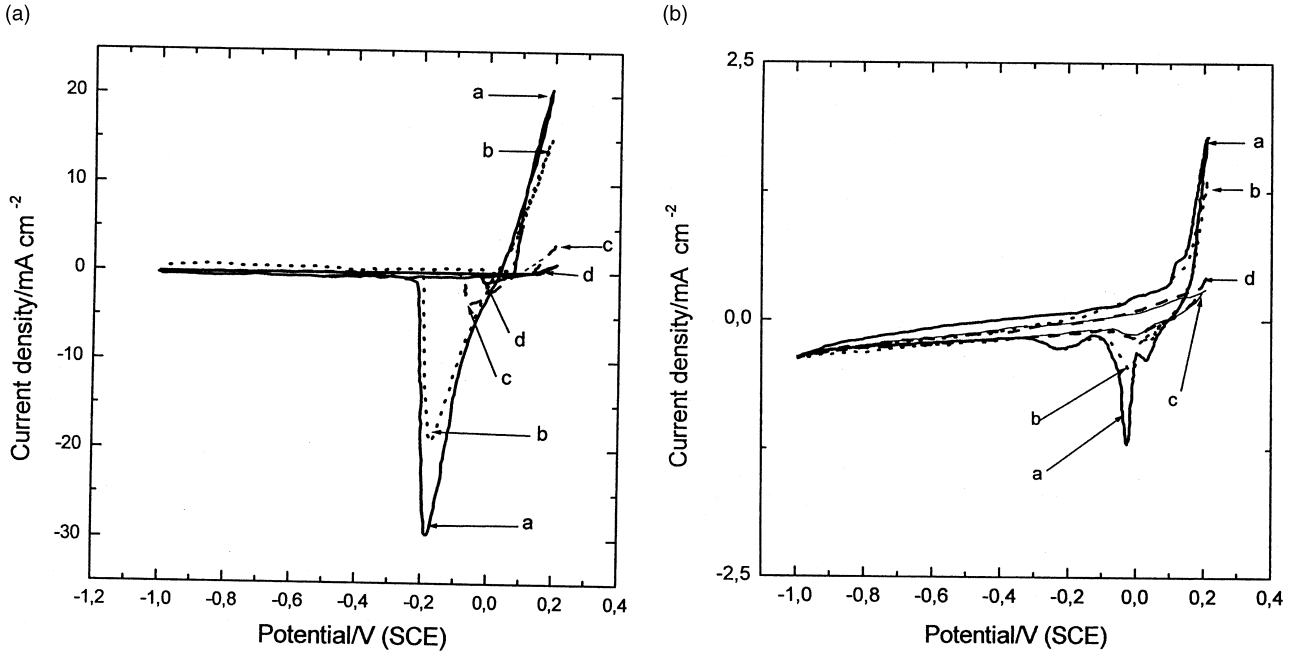

Fig. 4. Potentiodynamic cyclic polarisation curves at 20 mV s^{-1} with pure silver (A) and CAIII (B) in solutions with different chloride concentrations: (a) as Ringer's solution; (b) as saliva B; (c) as saliva E; (d) as saliva A (Table 1).

observed at potentials close to 0.1 V. However, lower current values than in the case of pure Ag are recorded.

In agreement with potentiodynamic results, CAIII potentiostatic current transients recorded at 0.09 V in a 0.028 M NaCl solution decrease monotonously with time. Accordingly, a passive behaviour was observed during the first potentiodynamic polarisation cycle (Figure 2). On the other hand current transients obtained with pure Ag at 0.09 and 0.12 V show a current increase to reach a maximum (Figure 5, curves a and b). Likewise it was observed previously [27] that the time and the height of the maximum depend on the potential.

3.1.2. *Effect of thiocyanate*

Experiments with 0.028 M NaCl with and without the addition of KSCN were made. A dramatic change in the reverse scan of the voltammogram can be observed when KSCN is added (Figure 6). The potential, shape

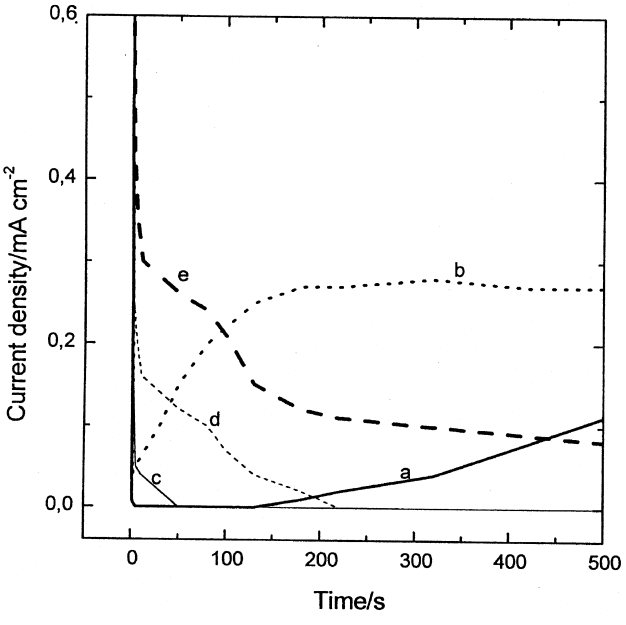

Fig. 5. Transient currents corresponding to pure silver in 0.028 M NaCl solutions without KSCN addition: (a) 0.09 V, (b) 0.12 V and with KSCN addition: (c) 0.33 g l^{-1} KSCN, 0.09 V; (d) 0.33 g l^{-1} KSCN, 0.12 V; (e) 0.5 g l^{-1} KSCN, 0.12 V.

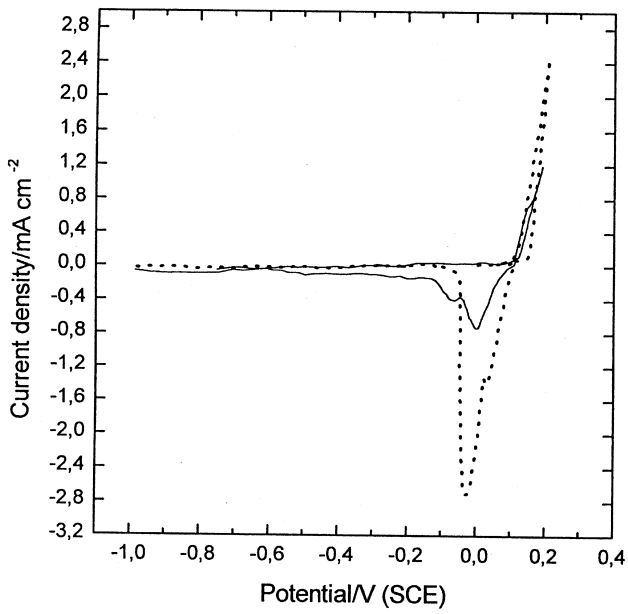

Fig. 6. Potentiodynamic cyclic polarisation curves at 20 mV s^{-1} with pure silver in 0.028 Nacl M solutions without KSCN addition (···) and with 0.33 g l^{-1} KSCN (—).

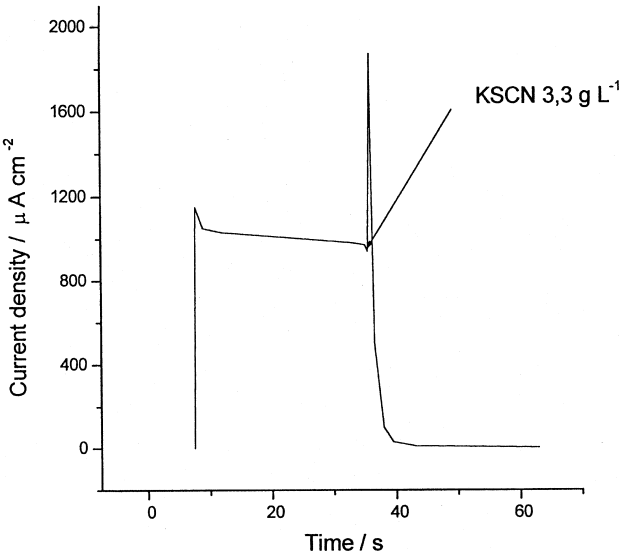

Fig. 7. Transient currents at 0.12 V corresponding to CAIII in 0.028 M NaCl solution showing the effect of KSCN addition (3.3 g l^{-1}, see the arrow).

and intensity of the cathodic peaks changed. Ag dissolution occurs at slightly lower potentials when both thiocyanate and chloride are present.

Potentiostatic current transients of pure silver recorded at 0.09 V in chloride solutions decrease monotonically with time. However, the current initially increases when SCN^- is added. At 0.12 V, in SCN^--containing solution (Figure 5, curves c–e) transient currents show a maximum followed by a current decrease. Lower values than the base chloride solutions were recorded at the end of the experiment. In agreement, Figure 7 shows the current decrease observed for CAIII when KSCN was added. A dark layer showing changing interference colours was observed at the end of the experiment.

It is worthy noticing that higher anodic current is recorded for the CAIII (Figure 2) in the −0.4–0.2 V potential range when a KSCN-containing saliva is used. This contribution becomes more significant after several cycles.

3.1.3. *Effect of carbonate and phosphate*

The shape of the CAIII voltammograms, does not change significantly when carbonate and phosphate ions are added in the concentration range indicated in Table 1. However, experiments made with phosphate-containing salivas (E and Er) and with chloride and phosphate solutions, show lower current values than those made with the base chloride solutions (Figures 2 and 4a). This accounts for the probably passive action of phosphate on the metal surface.

3.1.4. *Effect of fluoride*

The level of fluoride in natural saliva varies within a wide concentration range when fluoride-containing prophylactic products are used. The dissolution of pure Ag and CAIII was studied at different fluoride concentrations. It was found that the reduction peaks of pure Ag are higher, more anodic and sharper when fluoride is added. Voltammograms obtained with CAIII showed that fluoride yields higher dissolution of the metal.

3.2. *Dissolution of palladium*

Ag–15Pd oxidation currents can be related to either a selective dissolution of Ag or to a simultaneous stoichiometric dissolution of Ag and Pd [28, 29]. In order to elucidate which process is involved in each potential region, potentiostatic experiments with Ag–15Pd binary alloy were carried out in a 1 M KCl solution for 22 h. Table 2 shows the charge involved in the process. Afterwards, the Pd content of the solution (Pd/g) was determined through atomic absorption spectrometry and polarography analysis. The charge Q_{Pd} associated to (Pd/g) is also reported in Table 2.

The Pd profile within the metal coupon was determined through XPS analysis. The profile of the concentration of atomic Pd in the 200 Å outer layer of the alloy shows that Pd concentration increases towards the surface reaching a 40% level (Figure 8).

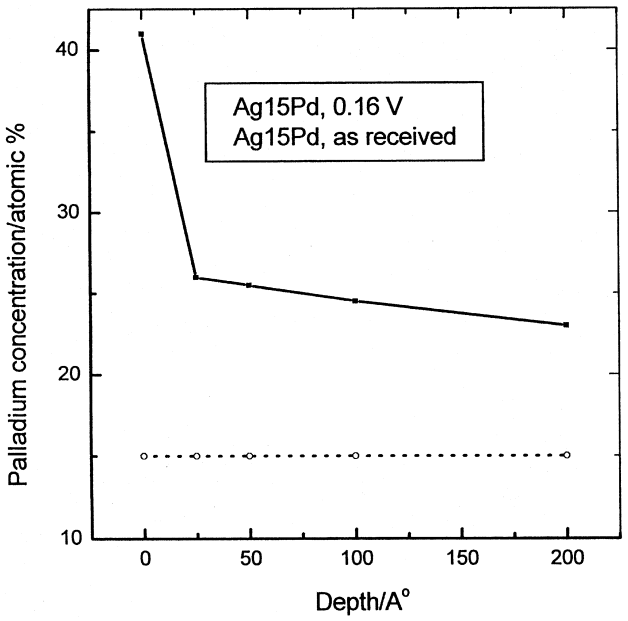

Fig. 8. Palladium concentration up to 200 Å depth in a Ag–15Pd alloy: after holding the electrode at 0.16 V for 22 h (—); control (- - -).

Table 2. Charge measurement (Q), Pd content in the solution (Pd), charge related to the Pd dissolution (Q_{Pd}), theoretic charge (Q_{PdTh}) and Pd selectivity coefficient (S_{Pd}) determined after the potentiostatic experiments with a Ag–15Pd alloy in 1 M KCl solution at different potentials

E vs SCE/V	Q/C	Pd/g	Q_{Pd}/C	Q_{PdTh}/C	S_{Pd}
0.16	0.0414	$<1.8\times10^{-6}$	$<3.3\times10^{-3}$	0.0108	<0.3
0.36	10.206	9.15×10^{-4}	1.66	2.66	0.62

4. Discussion

4.1. *Dissolution process of Ag–15Pd binary alloy*

The theoretic charge (Q_{PdTh}, Table 2) which should correspond to palladium dissolution if the dissolution was stoichiometric, can be calculated from Equation 1:

$$Q_{PdTh} = Q\left(\frac{n_{Pd}x_{Pd}}{n_{Ag}x_{Ag} + n_{Pd}x_{Pd}}\right) \quad (1)$$

Q = (current density × time) corresponding to potentiostatic experiments (Table 2), X_{Ag} and X_{Pd} are the atomic fractions of Ag and Pd in the bulk of the alloy, n_{Ag} and n_{Pd} the valences of Ag and Pd (+1 and +2, respectively).

Q_{PdTh} can be related to Q_{Pd}, the charge associated to the Pd content in the solution (Table 2), through a selectivity coefficient (S_{Pd}, Table 2) defined as:

$$S_{Pd} = \frac{Q_{Pd}}{Q_{PdTh}} \quad (2)$$

S_{Pd} is the relationship between the quantity of Pd in the solution and that corresponding to an ideal stoichiometric dissolution. Thus, if $S_{Pd} = 0$ (case I) there is a selective dissolution of Ag, if $S_{Pd} = 1$ (case II) there is a simultaneous dissolution of Ag and Pd in a stoichiometric relation (according to their relationship in the alloy composition), and if the value is between 0 and 1 there is a tendency to cases I or II according to the S_{Pd} value. The experiments were carried out with the Ag–15Pd binary alloy at 0.16 and 0.36 V, which correspond to a passive and an active potential region, respectively. Table 2 shows the selectivity coefficients of a Ag–15Pd in 1 M KCl solution obtained from the experiments. S_{Pd} values lower than 0.3 in the first case (0.16 V) and higher than 0.6 for the second (0.36 V) are related to a selective dissolution and simultaneous dissolution tendencies respectively. S_{Pd} lower than 0.3 could also be related to the dissolution of a microstructural phase with a higher Ag content than the average of the Ag–15Pd alloy (85%).

The preferential anodic dissolution of Ag should be expected to shift the electrode surface composition to higher Pd concentration [5]. In fact, the Pd level reaches 40% close to the surface (Figure 8). Due to the enrichment of the Pd content on the outer layers, a pseudo-passivation with an increase in the overvoltage is detected when the Ag-containing deposits are removed from the electrode surface.

4.2. *Influence of the anions on the electrochemical behaviour of Ag and Ag-based casting alloys*

4.2.1. *Effect of chloride and fluoride*

The electroformation of AgCl during the electrooxidation of pure Ag in NaCl solutions was interpreted through a complex model which implies the formation of adsorbed AgCl species at the submonolayer level, and the electrodissolution of Ag through the AgCl submonolayer diffusing out of the electrode as a complex ion ($AgCl_n^{-(n-1)}$). In the outer region $AgCl_n^{-(n-1)}$ participates in the nucleation and growth of AgCl followed by precipitation from the solution adjacent to the electrode. Fluoride enhances the action of chloride favouring the dissolution–precipitation process. Thus, the reaction mechanism could be described through the following sequence of reactions (where X is the halide) [27]:

$$Ag + X^- \Leftrightarrow AgX_{ad} + 1\,e^-$$

$$AgX_{ad} + (n-1)X^- \Leftrightarrow AgX_n^{-(n-1)}$$

$$AgX_n^{-(n-1)}(\text{electrode surface}) \Leftrightarrow AgX_n^{-(n-1)}(\text{solution})$$

$$x(AgX_n^{-(n-1)})(\text{solution}) \Leftrightarrow xAgX + [x(n-1)]X^-$$

$$xAgX(\text{solution}) \Leftrightarrow xAgX(\text{electrode surface})$$

A similar sequence may also correspond to the oxidation of Ag deposits formed on Ag–15Pd alloy surface after the cathodic scan. Dissolution of Ag from the alloy matrix requires a higher potential. The formation of $Pd(OH)_2$ film on Ag–15Pd alloy at 0.0 V seems to inhibit the dissolution process. When the halides are present the potential at which this film breaks down is dependent on the chloride concentration (Figure 4b) and may be related to the Pd dissolution according to the following overall reaction:

$$Pd + 4X^- \Leftrightarrow (PdX_4)^{2-} + 2\,e^-$$

Specific adsorption of anions that occurs in the double layer potential region may delay the electroadsorption of oxygen and consequently yield to an increase in the electrodissolution of the metal [28].

Cu is one of the casting alloy components and may adversely affect the corrosion resistance of the alloy [3]. In fact, the passivity region extends to more anodic potentials in the case of the Ag–Pd binary alloy. The Cu-rich phase of the casting alloy is probably selectively oxidised at potentials higher than −0.1 V. An anodic contribution, which is dependent on the chloride concentration, can be observed in this potential region (Figure 4b). It may be associated to CuCl and $CuCl_2^-$ formation. A sequence of reactions similar to that described for Ag could be used in this case [26].

Changes in *in vivo* environment (pH, redox potential, galvanic cells) may yield oxidation–reduction successive cycles and accumulation of Ag, Cu and their halides precipitated on the metal surface, on its surroundings or within the pores. These deposits are more active than the alloy matrix. The enrichment of soluble and insoluble Ag and Cu toxic corrosion products in the vicinity of the biomaterial *in vivo* may cause biocompatibility problems.

Cu and Ag were suggested as the most likely agents of succinic dehydrogenase (SDH) activity depression

related to cytotoxicity problems of Ag-based alloys [30]. The concentration level of Pd released from these alloys was low and did not show any effect.

4.2.2. *Effect of thiocyanate*

SCN^- concentration in natural saliva strongly depends on the habits of the patient. Thus, the average concentration of SCN^- in the natural saliva of smokers (0.09 g l^{-1}) is more than four times that of non-smokers (0.02 g l^{-1}) [7]. However, SCN^- level may be higher in crevices where the removal of the saliva is deficient.

The addition of SCN^- to the base chloride solution markedly affects the electrochemical behaviour of pure Ag. A dramatic change in the voltammograms and in the transient current records was caused by this anion, which seems to inhibit the dissolution of pure Ag and Ag-based casting alloys at potentials lower than 0.12 V. However, CAIII (which contains ca. 27% Cu) shows an increase in current density in the −0.4–0.2 V potential range when SCN^- is added to the plain chloride solution. A peak at −0.25 V is also observed after several cycles in saliva E (containing SCN^-, Figure 2). This contribution was detected neither in the voltammograms made with pure Ag (Figure 6) nor with the binary Ag–15Pd alloy. Cu-rich precipitates may be more affected by SCN^- than the alloy matrix. It was suggested that microsegregations or precipitates of Cu in the casting alloy could be mainly responsible for the corrosion of the Ag–Pd alloys [3]. Results of ESCA analysis revealed Cu and Ag dissolution at the metal surface of Cu-containing Ag–Pd alloys [2].

The film formed on pure Ag and Ag-based casting alloys during the potentiostatic experiments shows changing interference colours and is probably related to cuprous thiocyanate layer formation. It has been reported that this compound is formed on pure Cu at −0.4 V at pH 9 [29]. Thus, the following reaction probably takes place:

$$Cu + SCN^- \Leftrightarrow Cu(SCN) + 1\,e^-$$

Similarly, the formation of Ag(SCN) may account for the maximum observed in the transient currents (Figure 5) and for the changes of the voltammograms made with pure Ag when SCN^- is added (Figure 6).

$$Ag + SCN^- \Leftrightarrow Ag_{ad}(SCN) + 1\,e^-$$

Consequently, SCN^- ions favour tarnishing and pigmentation processes on the metal surface.

4.2.3. *Effect of bicarbonate and phosphate*

Bicarbonate and phosphate do not cause important changes on the electrochemical behaviour of Ag up to 0.2 V except for a reduction in the current density. At more anodic potentials $Cu_2(OH)_2CO_3$ is a stable compound formed in the presence of bicarbonate at pH higher than 6 [31, 32]. This anion is a component of salivas Er and E. The following reactions could take place on the Cu-containing Ag-based alloy:

$$2\,CuCl + 3\,H_2O \Leftrightarrow Cu_2(OH)_3Cl + Cl^- + 3\,H^+ + 2e^-$$

$$2\,CuCl + HCO_3^- + 2\,H_2O \Leftrightarrow Cu_2(OH)_2CO_3 + 3\,H^+ + 2\,Cl^- + 2\,e^-$$

$$CuCl(ad) \Leftrightarrow Cu^{+2} + Cl^- + 1\,e^-$$

4.2.4. *Effect of fluoride*

Though only a small amount of fluoride is present in natural saliva without external treatments, the concentration may be temporally high when fluoride-containing compounds are used in mouth rinses, dentifrices and gels as prophylactic agents to prevent caries development [33]. Potentiodynamic curves show that fluoride enhances the action of chloride anions and consequently, Ag dissolution increases as well as the tarnishing process.

5. Conclusions

Ag–15Pd binary alloy shows a selective dissolution tendency at potentials close to 0.16 V and simultaneous Ag and Pd dissolution at potentials higher than 0.36 V.

Ag-based casting alloy shows a complex electrochemical behaviour characterised by silver and copper current contributions which depend on the composition of the synthetic saliva. Ag deposits on the metal surface are more active than the matrix and render the alloy more susceptible to deterioration. Chloride, fluoride and thiocyanate have proved to affect corrosion, pigmentation and/or tarnishing processes.

The use of a normalised saliva is imperative to make comparisons of electrochemical results.

Acknowledgements

The authors acknowledge financial support from CONICET (PIP 4377796), the National Agency of Scientific and Technological Promotion (PICT 6782) and the University of La Plata, Argentina.

References

1. S. Sastri, T.K. Vaidyanathan and K. Mukherjee, *Metall. Trans. A* **13A** (1982) 313.
2. C. Bessing, M. Bergman and A. Thorén, *Dent. Mater.* **3** (1987) 153.
3. N.K. Sarkar, R.A. Fuys and J.W. Stanford, *J. Dent. Res.* **58** (1979) 1572.
4. R.C. Salvarezza, M.F.L. de Mele and H.A. Videla, *Biomaterials* **7** (1986) 297.
5. R.V. Weissman and P.J. Aragón, *J. Br. Endodontic Soc.* **9** (1986) 19.
6. S. Seltzer, D.B. Green, N. Weiner and F. DeRenzis, *Oral Surg.* **33** (1972) 589.
7. T.K. Vaidyanathan and A. Prasad, *J. Dent. Res.* **60** (1981) 707.
8. H. Loget, J. Lemounier and J.P. Frayret, Comportement électrochimique de quelques alliages dentaires à base d'argent utilisation

de la voltamétrie cyclique. Metaux, Corrosion, Industrie, 1982, no. 682, pp.1–12.
9. E. Quesada Castillo, MSc thesis, Universidad Nac. Gral San Martín, Argentina (1997).
10. E.J. Ewers and M.R. Thornber, *J. Electroanal. Chem.* **118** (1981) 275.
11. G.N. Jenkins, In 'Oral Physiology and Biochemistry', Limusa Press, Mexico, 1983, p. 303.
12. J.M. Meyer, *Corros. Sci.* **17** (1977) 971.
13. R.I. Holland, *Dent. Mater.* **8** (1992) 241.
14. A.J.W. Muller, F. Maessen and C.L. Davidson, *Dent. Mater.* **6** (1990) 63.
15. C. Baron, C.M. Marschoff and P.J. Aragon, *J. Life Sci.* **8** (1978) 105.
16. J.A. Di Girolamo, PhD thesis, Odontology College, Sao Pablo University, Brasil (1992).
17. T.K. Ross, D.A. Carter and D.C. Smith, *Corros. Sci.* **7** (1967) 373.
18. P.R. Mezger, M.A. Van't Hoff, M.M. Vrijhoef and E.J. Gravenmades, *J. Oral Rehabilitation* **16** (1989) 589.
19. V. Goehlich and M. Marek, *Dent. Mater.* **6** (1990) 103.
20. E. Angelini, P. Bianco, S. Mascellani and F. Zuchi, *J. Mater. Sci: Mater. Med.* **4** (1993) 142.
21. B.W. Darvell, *J. Oral Rehabilitation* **5** (1978) 41.
22. J. Brugirard, In 'Etude du comportement electrochimique des metaux et alliages dentaires', J. Prelat (ed.), Paris V°, 1970.
23. K. Arvidson and G. Johansson, *Scand. J. Dent. Res.* **93** (1985) 467.
24. E. Angelini, In 'Proceedings of the 14th International Corrosion Congress', Cape Town, South Africa, edited by International Corrosion Council, 1999, paper no. 11.1.
25. P. Novak, In 'Proceedings of the 14th International Corrosion Congress', Cape Town, South Africa, edited by International Corrosion Council, 1999, paper no.111.2.
26. M.R.G. de Chialvo, R.C. Salvarezza, D. Vasquez Moll and A.J. Arvia, *Electrochim. Acta* **30** (1985) 1501.
27. M.F.L. de Mele, R.C. Salvarezza, V.D. Vasquez Moll and A.J. Arvia, *J. Electrochem. Soc.* **133** (1986) 746.
28. J.A. Harrison and T.A. Whitfield, *Electrochim. Acta* **28** (1983) 1229.
29. M.G. Figueroa, M.F.L. de Mele, R.C. Salvarezza and A.J. Arvia *Electrochim. Acta* **32** (1987) 231.
30. J.C. Wataha, C.T. Malcolm and C.T. Hanks, *Intern. J. Prosthod.* **8** (1995) 9.
31. S.B. Adeloju, H.C. Hughes, *Corros. Sci.* **26** (1986) 851.
32. B. Little, P. Wagner, R. Ray and M. McNeil, *MTS J.* **24** (1990) 10.
33. M.F.L. de Mele and M.C. Cortizo, *J. Appl. Electrochim.* **30** (2000) 95.